

A perturbation theory for solvation thermodynamics: Dipolar–quadrupolar liquids

Dmitry V. Matyushov and Gregory A. Voth^{a)}

Department of Chemistry and Henry Eyring Center for Theoretical Chemistry, University of Utah, Salt Lake City, Utah 84112

(Received 28 January 1999; accepted 25 May 1999)

The thermodynamics of solvation of a dipole in hard sphere solvents with dipoles and quadrupoles is studied by using the Padé approximation for the perturbation expansion of the solvation chemical potential and compared to Monte Carlo simulations. Solvation chemical potentials, energies, and entropies of solvation are obtained at different dipolar and quadrupolar solvent strengths. The effect of nonlinear solvation is analyzed and found not to exceed 10% in the parameter range studied. An agreement between the simulations and the analytical theory is obtained by an empirical rescaling of the triple perturbation integrals of the perturbation expansion. This rescaling does not, however, provide a quantitatively correct partitioning of the solvation free energy into the energy and entropy of solvation. © 1999 American Institute of Physics. [S0021-9606(99)51531-6]

I. INTRODUCTION

Many solvents used in chemistry belong to the class of nondipolar liquids implying that the liquid molecules have zero permanent dipoles. The static dielectric constant of such solvents is close to the squared refractive index. A low dielectric constant does not necessarily mean a low solvation ability. Many chemical species can be solvated in nondipolar solvents because of the stabilization energy due to dispersion forces and nonzero higher solvent multipoles, of which the quadrupole moment is of primary importance.

The dielectric continuum modeling of solvation that is widely used for highly polar solvents has a very limited application to solvents with zero dipole moments and nonzero quadrupoles (quadrupolar solvents). The fundamental origin of its failure is the short range of quadrupolar interactions that do not directly contribute to the dielectric constant. Although the effect of quadrupoles on the solvent dielectric constant is significant,¹ it is reflected only in the Kirkwood *g*-factor that decreases due to breaking the angular dipole–dipole correlations with increasing quadrupolar strength.² Quadrupoles do not produce a macroscopic polarization of the solvent in an external field. The solvation free energy of a multipole solute in a nondipolar liquid is thus produced only by the induced solvent dipoles when calculated in the framework of continuum models. That this prediction is wrong has been clearly demonstrated in the recent measurements of the solvent reorganization energy for optical transitions of chromophores dissolved in nondipolar solvents.³ The solvent reorganization energy of electronic transitions reflecting solvation by only the nuclear degrees of freedom is zero when a nondipolar solvent is modeled by the dielectric continuum. Experiments on optical Stokes shifts in quadrupolar solvents show, on the contrary, quite substantial (300–500 cm⁻¹)³ reorganization energies, thus pointing to significant solvation by the solvent molecular quadrupoles.

Several attempts have been recently made to incorporate solvent quadrupoles into the continuum dielectric description of solvation.⁴ The continuum solvation energy is diminished by inclusion of the solvent quadrupoles owing to two factors. First, the dielectric constant of a polar solvent gets smaller because quadrupoles destroy dipole–dipole angular correlations, resulting in a decrease of the Kirkwood *g*-factor.^{1(b)} Second, the quadrupolar susceptibility makes a negative contribution to the continuum solvent response function.^{4(b)} A decrease of the solvation energy with the increase of the solvent quadrupole is at odds with molecular simulations of dipolar–quadrupolar fluids⁵ and leads to confusing results when applied to optical spectroscopy.⁶ A molecular description of solvation in nondipolar solvents is thus necessary.

Along these lines, reference interaction-site models (RISM)⁷ provide an important basis for calculating solvation energies, since they include all molecular multipoles by their construction. For such calculations, one needs the distribution of partial charges in both the solvent and the solute, as well as information about molecular geometries. This approach is difficult to implement for a variety of solvents given the scarcity of the input data and the necessity to solve a set of integral Ornstein–Zernike (OZ) equations for the site–site pair distribution functions.

Especially for treating spectroscopic data, for which changing the solvent is the common practice to probe the solvent effect, an approach for calculating solvation energetics from a few multipole moments of the solvent and the solute is highly desirable. An analytical procedure would also greatly simplify the data analysis. The present study is a development in that direction. The motivation of this paper is to develop a molecular treatment of solvation of a dipole in dipolar–quadrupolar solvents. Among different approaches to this problem suggested by equilibrium liquid state theories,⁸ we have chosen here a Padé truncation approach to the perturbation treatment of solvation.^{9,10} This method meets best our goal of creating an analytical framework for

^{a)}Electronic mail: voth@chemistry.chem.utah.edu

analyzing the solvent effect on optical transitions and electron transfer reactions in molecular liquids.

An alternative approach would be to use molecular integral equations with the hypernetted-chain (HNC)² or reference hypernetted-chain (RHNC)¹¹ closures for solvents with point dipoles and quadrupoles. In this approach, the OZ equation is expanded in spherical functions and closure relations are solved for each angular component. This approach is quite reliable in respect to the calculation of dielectric and thermodynamic properties of liquids without H-bonds.^{2(c)} The method is, however, relatively complicated and the development of alternative approaches is useful for applications and helps to better understand the multipolar solvation. In addition, we are interested here in obtaining the energy of reorganizing the solvent structure by the solute. This parameter is used as a means to calculate the internal energy and entropy of solvation and to test the general performance of the linear response theories. The latter information is hard to extract from integral equations involving angular projections,¹² but is straightforward in the perturbation approach.

This paper is organized as follows. In the next section, the model system of a dipolar solute in a solvent of hard sphere (HS) solvent molecules with point dipoles and quadrupoles is defined. In Sec. III, the perturbation expansion of the solvation chemical potential is developed and a Padé approximant is constructed. The analytical expressions are then tested against Monte Carlo (MC) simulations in Sec. IV where nonlinear solvation effects and the partitioning of the solvation free energy into the entropy and energy of solvation are also analyzed. Finally, Sec. V contains conclusions.

II. MODEL

The explicit model we employ here is that of a HS solute with a centered dipole moment m_0 in a solvent of HS molecules with dipoles and quadrupoles. The dipole moment is assumed to be the highest nonvanishing multipole of the solute (solute quadrupole is zero) and the consideration is limited to axially symmetric solvent molecules. We therefore have only two multipole parameters for the solvent: the dipole moment m and the quadrupole moment Q . (Q is the z, z -projection of the quadrupole tensor in the body-fixed axes frame.⁸) The interaction potential U_{0s} between the solute and the solvent reads as

$$U_{0s} = U_{0s}^{\text{HS}} + U_{0s}^p = \sum_j [u_{0s}^{\text{HS}}(0j) + u_{0s}^p(0j)], \quad (1)$$

where throughout below “0” and “s” stand for the solute and solvent, respectively. In Eq. (1), U_{0s}^{HS} is the solute–solvent HS repulsion and U_{0s}^p stands for the solute–solvent multipole interaction; the sum runs over the N solvent molecules. The multipole expansion of the solute–solvent interaction potential is given, in our model, by the sum of two terms,

$$u_{0s}^p(0j) = u_{0s}^{11}(0j) + u_{0s}^{12}(0j), \quad (2)$$

where the superscripts “1” and “2” refer to the first and the second multipole moments, respectively. Explicitly, we have

$$u_{0s}^{11}(01) = -(m_0 m / r_1^3) [3(\hat{\mathbf{s}}_0 \cdot \hat{\mathbf{r}}_1)(\hat{\mathbf{r}}_1 \cdot \hat{\mathbf{s}}_1) - (\hat{\mathbf{s}}_0 \cdot \hat{\mathbf{s}}_1)], \quad (3)$$

$$u_{0s}^{12}(01) = (3m_0 Q / 2r_1^4) [(\hat{\mathbf{s}}_0 \cdot \hat{\mathbf{r}}_1)(5(\hat{\mathbf{r}}_1 \cdot \hat{\mathbf{s}}_1)^2 - 1) - 2(\hat{\mathbf{s}}_0 \cdot \hat{\mathbf{s}}_1)(\hat{\mathbf{r}}_1 \cdot \hat{\mathbf{s}}_1)], \quad (4)$$

where $\hat{\mathbf{s}}_0$ and $\hat{\mathbf{s}}_1$ are the unit vectors determining orientations of the solute and solvent ($j=1$) molecules, and $\hat{\mathbf{r}}_1 = \mathbf{r}_1 / r_1$.

The solvent–solvent interaction potential,

$$U_{ss} = U_{ss}^{\text{HS}} + U_{ss}^p = \frac{1}{2} \sum_{j \neq k} [u_{ss}^{\text{HS}}(jk) + u_{ss}^p(jk)], \quad (5)$$

also includes the HS repulsion, u_{ss}^{HS} , and the multipole interaction, u_{ss}^p . The latter is given by the sum of three terms,

$$u_{ss}^p(jk) = u_{ss}^{11}(jk) + u_{ss}^{\text{DQ}}(jk) + u_{ss}^{22}(jk). \quad (6)$$

The dipole–dipole potential, u_{ss}^{11} , between the solvent molecules derives from Eq. (3) by replacing the solute by a solvent molecule. The quadrupole–quadrupole interaction reads as⁸

$$u_{ss}^{22}(12) = (3Q^2 / 4r_{12}^5) [1 - 5(\hat{\mathbf{s}}_1 \cdot \hat{\mathbf{r}}_{12})^2 - 5(\hat{\mathbf{s}}_2 \cdot \hat{\mathbf{r}}_{12})^2 + 2(\hat{\mathbf{s}}_1 \cdot \hat{\mathbf{s}}_2)^2 + 35(\hat{\mathbf{s}}_1 \cdot \hat{\mathbf{r}}_{12})^2 (\hat{\mathbf{s}}_2 \cdot \hat{\mathbf{r}}_{12})^2 - 20(\hat{\mathbf{s}}_1 \cdot \hat{\mathbf{r}}_{12})(\hat{\mathbf{s}}_2 \cdot \hat{\mathbf{r}}_{12})(\hat{\mathbf{s}}_1 \cdot \hat{\mathbf{s}}_2)]. \quad (7)$$

The dipole–quadrupole solvent–solvent potential u_{ss}^{DQ} in Eq. (6) is a sum of interactions between the two multipoles: $u_{ss}^{\text{DQ}}(12) = u_{ss}^{12}(12) + u_{ss}^{21}(12)$. The potential

$$u_{ss}^{\text{DQ}}(12) = (3mQ / 2r_{12}^4) ((\hat{\mathbf{s}}_2 \cdot \hat{\mathbf{r}}_{12}) - (\hat{\mathbf{s}}_1 \cdot \hat{\mathbf{r}}_{12})) \times [5(\hat{\mathbf{s}}_1 \cdot \hat{\mathbf{r}}_{12})(\hat{\mathbf{s}}_2 \cdot \hat{\mathbf{r}}_{12}) + 1 - 2(\hat{\mathbf{s}}_1 \cdot \hat{\mathbf{s}}_2)] \quad (8)$$

is therefore symmetric in respect to interchange of the solvent molecules. This symmetry does not exist for the solute–solvent dipole–quadrupole interaction, since the solute quadrupole is assumed to be equal to zero.

The interaction potentials in Eqs. (1)–(8) give a complete definition of the present model system. In the next section, we derive the perturbation expansion for the solvation chemical potential in terms of the multipolar interaction potentials between the solute and the solvent, u_{0s}^p , and between the solvent molecules, u_{ss}^p . The reference system is the liquid of solvent hard spheres with the immersed solute hard sphere core. In order to generate an infinite perturbation series in solvent dipolar and quadrupolar strengths, we form a Padé approximant composed of the two first nonvanishing perturbation terms.

III. THERMODYNAMIC PERTURBATION EXPANSION

The excess chemical potential μ_p relative to the free energy of inserting the solute HS core into the solvent can be derived from the thermodynamic coupling parameter integration,⁸

$$\mu_p = \rho \int_0^1 d\lambda \int u_{0s}^p(01) g_{0s}(\lambda; 01) d\Gamma_1 (d\Omega_0 / 4\pi). \quad (9)$$

Here λ is the solute–solvent coupling parameter and the integration is carried out over the coordinates and orientations of the solvent molecules (Γ) and the orientations of the sol-

ute dipole (Ω_0). The function $g_{0s}(\lambda;01)$ is the solute–solvent pair distribution function (PDF) at the coupling strength λ , while ρ is the solvent number density. A perturbation expansion for μ_p is obtained by expanding $g_{0s}(\lambda;01)$ in the solute–solvent and solvent–solvent multipole interaction potentials relative to the reference system composed of the solute and solvent hard spheres.^{10(a)(b)} The expansion will be truncated after the first two nonvanishing terms used to build a Padé approximant.

The first nonvanishing expansion term follows from the first order expansion $g_{0s}(\lambda;01) \approx g_{0s}^{(0)}(r_1) - \lambda \beta u_{0s}^p(01) g_{0s}^{(0)}(r_1)$ which, after substitution into Eq. (9), yields

$$\beta \mu_p^{(2)} = -(\beta m_0^2 / \sigma^3) [y_d I_4^{(2)} + y_q I_6^{(2)}], \quad (10)$$

with

$$I_n^{(2)} = (n-1) \int_0^\infty \frac{dx}{x^n} g_{0s}^{(0)}(x), \quad (11)$$

and $g_{0s}^{(0)}(x)$ is the HS solute–solvent PDF. In Eq. (10), σ is the HS diameter of the solvent molecules and we have introduced the density of solvent quadrupoles,

$$y_q = (2\pi/5) \rho^* (Q^*)^2, \quad (12)$$

by analogy with the well-known density of the solvent dipoles,⁸

$$y_d = (4\pi/9) \rho^* (m^*)^2, \quad (13)$$

where $\rho^* = \rho \sigma^3$, $(m^*)^2 = \beta m^2 / \sigma^3$, and $(Q^*)^2 = \beta Q^2 / \sigma^5$. In contrast to the dipoles density y_d that depends only on the solvent number density ρ and the dipole moment (the common σ^3 factor cancels out), the quadrupoles density y_q includes also the HS diameter σ . This is because the quadrupole interacts with the gradient of the electric field and not with the field itself as in the dipole case.

The second order expansion contains two-particle terms of the type $\langle u_{0s}^p(01)^3 \rangle_\omega$ and three particle terms of the form $\langle u_{0s}^p(01) u_{ss}^p(12) u_{0s}^p(20) \rangle_\omega$, where $\langle \dots \rangle_\omega$ denotes the angular average over the solvent and solute orientations. The $\langle u_{0s}^p(01)^3 \rangle_\omega$ term disappears for symmetry reasons. Note that this does not happen for the perturbation expansion in pure liquids since the dipole–quadrupole potential (8) is symmetric with respect to the particle interchange and the term $\langle u_{ss}^{\text{DQ}}(01)^2 u_{ss}^p(01) \rangle_\omega$ is nonzero.⁵ The second order expansion term contains therefore only the three-particle contributions and can be written as follows:

$$\beta \mu_p^{(3)} = (\beta m_0^2 / \sigma^3) [y_d^2 I_{\text{DDD}}^{(3)} + y_d y_q I_{\text{DDQ}}^{(3)} + y_q^2 I_{\text{DQQ}}^{(3)}]. \quad (14)$$

The three-particle perturbation integrals $I_{\text{DDD}}^{(3)}$, $I_{\text{DDQ}}^{(3)}$, and $I_{\text{DQQ}}^{(3)}$ are responsible for the three-particle correlations: dipole–dipole–dipole (DDD), dipole–dipole–quadrupole (DDQ), and dipole–quadrupole–quadrupole (DQQ). The perturbation integrals are functions of the solvent reduced density, ρ^* , and the reduced distance of the solute–solvent closest approach, $r_{0s} = R_0 / \sigma + 0.5$, where R_0 is the solute radius. The analytical expressions for the three-particle perturbation integrals, as well as polynomial fits of both the two-particle and three-particle integrals, are explicitly given in Appendix A.

The Padé approximant can be built using Eqs. (10) and (14) as follows:

$$\mu_p = \mu_p^{(2)} / [1 - \mu_p^{(3)} / \mu_p^{(2)}]. \quad (15)$$

A comparison to the simulations of solvation in purely dipolar solvents^{10(c)} and the simulation data presented here both show that the Padé approximation (PA) somewhat overestimates the solvation energy. This seems to be a general problem of the Padé truncation of perturbation series, since the same trend is seen for the free energy of homogeneous multipolar fluids.^{5(b),8} Since the main error is in the denominator term $\mu_p^{(3)} / \mu_p^{(2)}$ in Eq. (15),^{5(b)} an agreement with simulations may be achieved by introducing the empirical factors κ_p , κ_q , and κ_{pq} correcting for errors in estimating the effect of many-body multipolar correlations on solvation. Note that the PA accounts only for the three-particle correlations attempting to include all higher order terms by constructing a geometric series. With the correction factors included, we will define the solvation chemical potential as follows:

$$\mu_p^{\text{P}} = -\frac{m_0^2}{\sigma^3} \frac{f^{(2)}}{1 + f^{(3)} / f^{(2)}}, \quad (16)$$

where

$$f^{(2)} = y_d I_4^{(2)} + y_q I_6^{(2)}, \quad (17)$$

$$f^{(3)} = y_d^2 \kappa_d I_{\text{DDD}}^{(3)} + y_d y_q \kappa_{dq} I_{\text{DDQ}}^{(3)} + y_q^2 \kappa_q I_{\text{DQQ}}^{(3)}. \quad (18)$$

The correction factor κ_d was obtained in the previous paper dealing with purely dipolar HS solvents.^{10(c)} Therefore, we need to determine κ_q and κ_{dq} . As the first step, we will generate solvation internal energies u_p from MC simulations in quadrupolar solvents with zero dipole moments. This provides information about κ_q . Then, with κ_q and κ_d in hand, we will extract κ_{dq} from simulations of solvation in solvents with nonzero dipole and quadrupole moments.

IV. RESULTS

A. Monte Carlo simulations

The MC simulations were carried out for a dipolar solute in a fluid of HS solvent molecules with point dipoles and linear quadrupoles. The solute was initially inserted into a

TABLE I. Solvation energy $\langle U_{0s}^p \rangle$, the second moment $\langle (\delta U_{0s}^p)^2 \rangle$, and the nonlinear solvation parameter χ_{NL} [Eq. (21)] from MC simulations at $r_{0s} = 1.0$, $\rho^* = 0.8$, $\beta m_0^2 / \sigma^3 = 10$.

$(Q^*)^2$	$(m^*)^2 = 0.0$			$(m^*)^2 = 1.0$		
	$-\beta \langle U_{0s}^p \rangle$	$\beta^2 \langle (\delta U_{0s}^p)^2 \rangle^a$	χ_{NL}	$-\beta \langle U_{0s}^p \rangle$	$\beta^2 \langle (\delta U_{0s}^p)^2 \rangle^a$	χ_{NL}
0.25	8.24 ± 0.01	8.67 ± 0.01	1.05	21.91 ± 0.05	21.41 ± 0.04	0.98
0.50	14.67 ± 0.04	15.50 ± 0.20	1.06	30.16 ± 0.04		
0.75	18.99 ± 0.04	18.51 ± 0.08	0.98	29.35 ± 0.04	28.25 ± 0.10	0.96
1.00	23.07 ± 0.03	20.34 ± 0.10	0.88	32.80 ± 0.15	32.71 ± 0.50	1.00
1.25	26.18 ± 0.09	24.66 ± 0.21	0.94	34.86 ± 0.12	35.91 ± 0.57	1.03
1.50	29.03 ± 0.25	25.98 ± 0.55	0.90	35.12 ± 0.18	37.32 ± 1.56	1.06
1.75	30.77 ± 0.08	26.48 ± 0.22	0.86	36.12 ± 0.06	35.32 ± 0.62	0.98
2.00	31.76 ± 0.25			37.92 ± 0.78		

^aEmpty entries imply that we could not reach a stationary value after 9×10^5 trial moves.

TABLE II. Solvation energy $\langle U_{0s}^p \rangle$ and the second moments $\langle (\delta U_{0s}^p)^2 \rangle$ and $\langle \delta U_{0s}^p \delta U_{ss}^p \rangle$ from MC simulations at $r_{0s}=1.4$, $\rho^*=0.8$, $\beta m_0^2/\sigma^3=10$, $\beta Q^2/\sigma^5=0.5$. Also given are the nonlinear solvation parameter χ_{NL} , internal energy of solvation, e_p , solvation entropy, s_p , and the chemical potential of solvation, μ_p .^a

$(m^*)^2$	$-\beta\langle U_{0s}^p \rangle$	$\beta^2\langle (\delta U_{0s}^p)^2 \rangle$	$\langle \delta U_{0s}^p \delta U_{ss}^p \rangle_1$	χ_{NL}	$-\beta e_p$	$-s_p/k_B$	$-\beta\mu_p$
0.00	2.47±0.01	2.89±0.01		1.170			1.24
0.25	5.45±0.01	5.01±0.01	2.93±0.04	0.919	3.99	1.26	2.73
0.50	6.14±0.01	5.96±0.01	4.36±0.04	0.942	3.80	0.74	3.06
0.75	7.00±0.001	7.54±0.02	4.17±0.08	1.077	4.92	1.42	3.50
1.00	7.65±0.01	7.21±0.01	4.25±0.20	0.938	5.47	1.65	3.77
1.25	8.23±0.01	7.90±0.01	5.77±0.10	0.960	5.35	1.23	4.12
1.50	8.61±0.03	8.11±0.03	7.36±0.14	0.942	4.93	0.63	4.30
1.75	8.88±0.01	8.50±0.02	6.99±0.04	0.957	5.39	0.95	4.45
2.00	9.13±0.02	8.33±0.06	7.65±0.30	0.912	5.31	0.74	4.57
2.25	9.34±0.01	9.06±0.03	7.45±0.17	0.970	5.62	0.95	4.67
2.50	9.52±0.01	9.41±0.35	8.01±0.12	0.988	5.52	0.76	4.76
3.00	9.84±0.02	9.75±0.03	7.50±0.20	0.991	6.09	1.17	4.92

^aStandard deviations are measured on the last 10^5 trial moves of the simulation runs.

cubic simulation cell with the solvent molecules placed on the fcc lattice with random orientations. In order to avoid overlap with the solvent molecules, the solute size was gradually increased to the desired magnitude in the course of standard MC runs, as described in previous publications.^{10(c),13} Periodic boundary conditions with the minimum image convention¹⁴ were employed for a cubic simulation box of side-length L . The long-ranged multipolar interactions were truncated beyond the cutoff distance $R_c = L/2$. The reaction-field (RF) long-range corrections with the continuum dielectric constant $\epsilon_{RF}=1000$ have been adopted for the dipole–dipole interaction potential. The simulation results are usually reasonably insensitive to the choice of ϵ_{RF} , and values of ϵ_{RF} higher than the dielectric constant of the pure solvent ensure better convergence of dielectric and thermodynamic parameters.¹⁵ No corrections have been made for the truncation of more short-ranged dipole–quadrupole and quadrupole–quadrupole interactions, which is the usual approximation for treating dense liquids with quadrupoles.^{16,17}

The simulations were performed with $N=500$ solvent molecules on the SGI Challenge L-IRIX 6.5 194 MHz processor. About 40 hours of CPU time was needed for each 10^5 trial moves (translations and rotations) per particle. The first and the second moments of the solute–solvent interaction potential, $\beta\langle U_{0s}^p \rangle$ and $\beta^2\langle (\delta U_{0s}^p)^2 \rangle$, as well as the mixed moment $\beta^2\langle \delta U_{0s}^p \delta U_{ss}^p \rangle$, were measured on the last 10^5 trial moves. The moment $\beta^2\langle \delta U_{0s}^p \delta U_{ss}^p \rangle$ is the slowest converging quantity and, depending on its rate of convergence, $(5-9)\times 10^5$ trial moves were carried out. The simulation results at different solute and solvent parameters are listed in Tables I–II.

B. Linear response approximation

The excess chemical potential μ_p^p in Eq. (16) is proportional to the squared solute dipole moment. The perturbation expansion of Sec. III is, therefore, restricted to the linear response approximation (LRA).¹⁸ Before used, the LRA hypothesis should be tested on MC simulations. This can be achieved by applying some thermodynamic relations following from the linear solvent response.^{10(c)} First, the solvation

chemical potential μ_p is simply related to the average interaction energy of the solute–solvent multipolar interaction,

$$2\mu_p = e_{0s}, \quad e_{0s} = \langle U_{0s}^p \rangle. \quad (19)$$

The average interaction energy can, in turn, be found from the second moment of the solute–solvent potential,

$$e_{0s} = \beta \langle (\delta U_{0s}^p)^2 \rangle. \quad (20)$$

The two equivalent ways of calculating e_{0s} provide a means of testing the LRA. The parameter

$$\chi_{NL} = \beta \frac{\langle (\delta U_{0s}^p)^2 \rangle}{\langle U_{0s}^p \rangle}, \quad (21)$$

serves as a measure of deviation of the solvent response from the LRA prediction $\chi_{NL}=1$. The nonlinear solvation parameters for dipolar–quadrupolar solvents of various polarity are listed in Tables I and II from which one can infer that the LRA approximation holds within 10% in the range of parameters studied. The comparison of two columns in Table I shows that purely quadrupolar solvents tend to produce a more nonlinear response than solvents with nonzero dipolar components.

C. Solvation thermodynamics

The mixed solute–solvent/solvent–solvent moment $\langle \delta U_{0s}^p \delta U_{ss}^p \rangle$ enables one to extract the internal energy, e_p , and entropy, s_p , of solvation. Here, δU_{0s}^p and δU_{ss}^p are fluctuations of the solute–solvent and solvent–solvent multipolar potentials, respectively. A route to the thermodynamic solvation potentials is provided by the fundamental relation¹²

$$e_p = e_{0s} + e_{ss}, \quad (22)$$

representing the internal solvation energy as the sum of the average solute–solvent interaction energy, e_{0s} , and the change of the solvent–solvent interaction energy, e_{ss} , induced by the solute (the energy of solvent reorganization) with respect to the bulk solvent. The latter quantity is given in the LRA as^{10(c)}

$$e_{ss} = -(\beta/2)\langle \delta U_{0s}^p \delta U_{ss}^p \rangle. \quad (23)$$

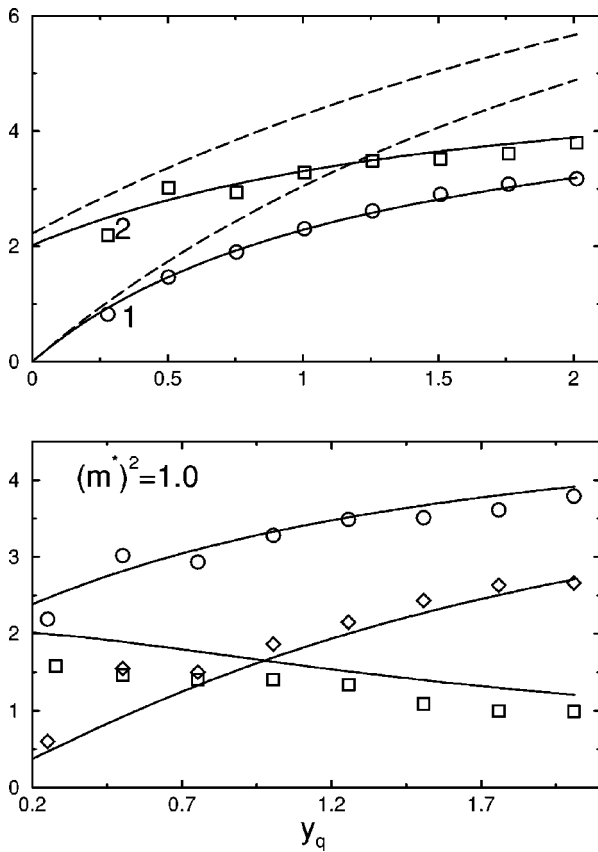


FIG. 1. Reduced average solute-solvent interaction energy $-(\sigma^3/m_0^2)\langle U_{0s}^p \rangle \times \langle U_{0s} \rangle$ versus the quadrupolar density y_q at $r_{0s}=1.0$, $\rho^*=0.8$. In the upper panel, the Padé approximation is shown without (dashed lines) and with (solid lines) the correction factors κ_q , κ_d , and κ_{dq} [Eqs. (27)–(29)] for $(m^*)^2=0.0$ (1) and $(m^*)^2=1.0$ (2). Points represent the simulation results. In the lower panel, the solute-solvent interaction energy (circles) is split into the component due to solvent dipoles (squares) and quadrupoles (diamonds). Solid lines represent Padé results given by Eqs. (16), (36), and (37).

If we introduce the dimensionless parameter

$$\chi_s = \beta \frac{\langle \delta U_{0s}^p \delta U_{ss}^p \rangle}{\langle U_{0s}^p \rangle}, \quad (24)$$

then the internal energy, e_p , and entropy, s_p , of solvation read as

$$e_p = e_{0s}(1 - \chi_s/2), \quad (25)$$

$$Ts_p = (e_{0s}/2)(1 - \chi_s). \quad (26)$$

With the above general thermodynamic relations in hand, we can now analyze our MC data. We start with the average solute-solvent interaction energy in order to determine the correction coefficients κ_q and κ_{dq} . According to the LRA, one needs to compare e_{0s} from simulations with $2\mu_p^p$. Results for purely quadrupolar solvents (Table I) give us κ_q . Fortunately, the correction coefficient is independent of y_q and a simple approximation is possible. The correction factor,

$$\kappa_q = 2 + 1/(d^5 + 2), \quad (27)$$

was found to fit the Padé form to the simulation results (Fig. 1) over the whole range of Q^* values studied. Here d is the

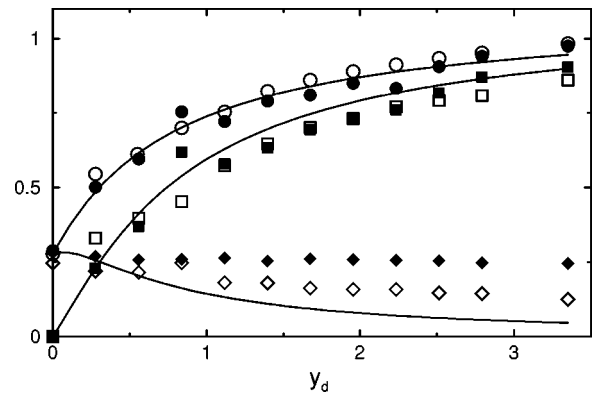


FIG. 2. $-(\sigma^3/m_0^2)\langle U_{0s}^p \rangle$ (open circles) and $(\beta\sigma^3/m_0^2)\langle (\delta U_{0s}^p)^2 \rangle$ (filled circles) versus y_d at $r_{0s}=1.4$ and $\rho^*=0.8$. Open and filled squares refer to the dipole-dipole component of $-(\sigma^3/m_0^2)\langle U_{0s}^p \rangle$ and $(\beta\sigma^3/m_0^2)\langle (\delta U_{0s}^p)^2 \rangle$, respectively. Open and filled diamonds indicate the dipole-quadrupole components of the same moments. Lines represent the Padé approximation for the solvation energy e_{0s} (upper curve) and its partitioning into the dipole-dipole [e_{0s}^{11} , medium curve, Eq. (36)] and dipole-quadrupole [e_{0s}^{12} , lower curve, Eq. (37)] components. Points are the simulation results.

ratio of the solute and solvent diameters, $d=2R_0/\sigma$. In the previous study of solvation by purely dipolar liquids,^{10(c)} the correction factor κ_p was found to be independent of the dipolar density y_d and can be given by the relation [Eq. (36) in Ref. 10(c)]

$$\kappa_d = 1 + [d/(d+1)]^2. \quad (28)$$

With κ_q and κ_d known the internal solvation energies in solvents with nonzero dipoles and quadrupoles (Tables I–II) can be fitted to κ_{dq} in the form

$$\kappa_{dq} = 2 - d^5/(d^5 + 2). \quad (29)$$

The quality of the fit is illustrated in Figs. 1–2.

It is always instructive to know the partitioning of the solute-solvent solvation energy e_{0s} into the components arising from different interaction potentials. In the present model, these are dipole-dipole and dipole-quadrupole interactions. This partitioning is straightforward from computer simulations, but needs a separate derivation in the perturbation approach. The solvation energies,

$$e_{0s}^{11} = \left\langle \sum_j u_{0s}^{11}(j) \right\rangle \quad \text{and} \quad e_{0s}^{12} = \left\langle \sum_j u_{0s}^{12}(j) \right\rangle, \quad (30)$$

can be calculated from the generating functional

$$\begin{aligned} & \exp[-\beta\mu_p(x,y)] \\ &= \int d\Gamma_1^N(d\Omega_0/4\pi) \exp[-\beta U(x,y) - \beta U]. \end{aligned} \quad (31)$$

Here $U = U_{0s} + U_{ss}$,

$$U(x,y) = U_{0s}(x,y) + U_{ss}(x,y), \quad (32)$$

$d\Gamma_1^N = d\Gamma_1 \dots d\Gamma_N$, and $U(x,y)$ is obtained by scaling of the solvent multipoles $m \rightarrow xm$, $Q \rightarrow yQ$ in the potential energy U . From Eq. (31), it is easy to see that

TABLE III. Coefficients of the third order density polynomials $a(\rho^*)$, $b(\rho^*)$, $c(\rho^*)$, and $d(\rho^*)$ in the fitting functions for the perturbation integrals in Eqs. (A8)–(A10).

n	$I_6^{(2)}$				$I_{DDQ}^{(3)}$				$I_{DQQ}^{(3)}$			
	a	b	c	d	a	b	c	d	a	b	c	d
0	1	0	0	0	4/5	-1/2	0	1/32	5/24	0	-5/64	1/128
1	0.586	1.062	-0.970	0.241	0.365	0.652	-1.510	0.044	0.936	-1.629	10.35	-6.712
2	-1.390	4.608	-4.134	1.194	-0.656	4.779	-7.378	3.770	0.330	0.509	-20.530	13.990
3	0.776	-2.964	3.798	-1.393	0.179	-2.297	5.087	-2.928	-0.216	1.005	10.30	-7.512

$$e_{0s}^{11} = \left. \frac{\partial \mu_p(x,y)}{\partial x} \right|_{x,y=0}, \quad e_{0s}^{12} = \left. \frac{\partial \mu_p(x,y)}{\partial y} \right|_{x,y=0}. \quad (33)$$

In order to obtain the generating functional $\mu_p(x,y)$, we need to construct the Padé approximant for the potential $U + U(x,y)$. This procedure is straightforward along the lines of Sec. III from which $\mu_p(x,y)$ is given by Eq. (16) with the coefficients (Appendix B)

$$f^{(2)}(x,y) = (1+x)^2 y_d I_4^{(2)} + (1+y)^2 y_q I_6^{(2)} \quad (34)$$

and

$$f^{(3)}(x,y) = (1+x)^2 (1+x^2) y_d^2 \kappa_d I_{DDD}^{(3)} + (1+y)(1+x)(1+xy) y_d y_q \kappa_{dq} I_{DDQ}^{(3)} + (1+y)^2 (1+y^2) y_q^2 \kappa_q I_{DQQ}^{(3)}. \quad (35)$$

From Eqs. (33)–(35) we have

$$e_{0s}^{11} = -\frac{m_0^2}{\sigma^3} \frac{2y_d I_4^{(2)} + 2y_d^2 \kappa_d I_{DDD}^{(3)} + y_d y_q \kappa_{dq} I_{DDQ}^{(3)}}{(1+f^{(3)}/f^{(2)})^2} \quad (36)$$

and

$$e_{0s}^{12} = -\frac{m_0^2}{\sigma^3} \frac{2y_q I_6^{(2)} + 2y_q^2 \kappa_q I_{DQQ}^{(3)} + y_d y_q \kappa_{dq} I_{DDQ}^{(3)}}{(1+f^{(3)}/f^{(2)})^2}. \quad (37)$$

In the lower panel in Fig. 1, we have shown the partitioning of the solute–solvent interaction energy into the components due to the solvent dipoles and quadrupoles. The simulation results (points) are compared to the analytical predictions given by Eqs. (36) and (37) (solid lines). As is seen from the figure, the two solvation component coincide at $(m^*)^2 = 1.0$ and $(Q^*)^2 = 0.5$. This implies that quadrupoles are approximately twice as effective in solvating a dipole compared to solvent dipoles, at $r_{0s} = 1$. This does not, however, mean that solvation in polar liquids is dominated by quadrupoles. The value of the reduced dipole moment as much as $(m^*)^2 \approx 5.0$ can be achieved in such polar solvents as acetonitrile ($m = 3.9D$, $\sigma = 4.14 \text{ \AA}$). On the other hand, very few commonly used solvents have the reduced quadrupole moment as high as $(Q^*)^2 = 0.5$ [e.g., for benzene $(Q^*)^2 = 0.42$; for carbon dioxide $(Q^*)^2 = 0.68$; for ethanol $(Q^*)^2 = 0.46$; for dimethylsulfoxide $(Q^*)^2 = 0.67$]. Therefore, for polar solvents like acetonitrile [$(m^*)^2 = 5.2$, $(Q^*)^2 = 0.12$], acetone [$(m^*)^2 = 1.8$, $(Q^*)^2 = 0.22$], nitromethane [$(m^*)^2 = 3.76$, $(Q^*)^2 = 0.44$] the dipolar solvation mechanism will be prevailing. For less polar

solvents, like tetrahydrofuran [$(m^*)^2 = 0.56$, $(Q^*)^2 = 0.20$], quadrupoles and dipoles should equally contribute to the solvation energetics.

The partitioning of the solvation energy into the quadrupolar and dipolar components depends, however, on the solute size. The upper panel in Fig. 2 shows the first ($\langle U_{0s}^p \rangle$, open circles) and the second ($\langle (\delta U_{0s}^p)^2 \rangle$, filled circles) moments of the solute–solvent potential versus the solvent dipolar strength. The splitting of both $\langle U_{0s}^p \rangle$ and $\langle (\delta U_{0s}^p)^2 \rangle$ into the contributions from the dipole–dipole (squares) and dipole–quadrupole (diamonds) potentials is also shown. We see that for the solute of the size $r_{0s} = 1.4$ the solvation energies arising from the interaction of the solute with the solvent dipoles and solvent quadrupoles are approximately equal for the close magnitudes of the dipolar ($y_d \approx 0.5$) and quadrupolar ($y_q \approx 0.5$) polarity parameters. The quadrupoles are thus less effective in creating the solvation stabilization compared to the case $r_{0s} = 1.0$ shown in Fig. 1. This is because quadrupolar forces die off faster than dipolar forces. As a result, the relative impact of quadrupolar solvation diminishes with increasing solute size. The ratio of the quadrupolar to dipolar solvation energies varies approximately as

$$2.0 \frac{(Q^*)^2}{(m^*)^2} r_{0s}^{-4/3}. \quad (38)$$

Figure 2 indicates that the quadrupolar solvation energy (diamonds) decays with increasing y_d . This reflects increasing breaking of the quadrupolar orientational order by the solvent dipoles resulting in less effective quadrupolar solvation. Figure 2 also illustrates the issue of nonlinear solvation effects. The first and the second moments are close to each other and the deviation of the nonlinear solvation parameter χ_{NL} [Eq. (21)] from unity (Tables II and III) does not exceed 10%. It is also seen from Fig. 2 that the quadrupolar component of the average solute–solvent energy (diamonds) shows a more pronounced nonlinear solvation effect compared to the dipolar component.

Equations (22)–(26) provide a route to calculate the internal energy and entropy of solvation. The key parameter here is the energy of the solvent reorganization that, in the LRA, is connected to the moment $-\beta \langle \delta U_{0s}^p \delta U_{ss}^p \rangle$ by Eq. (23). This parameter and the two first moments of the solute–solvent potential are listed at $r_{0s} = 1.4$, $\rho^* = 0.8$, $(Q^*)^2 = 0.5$, and varying $(m^*)^2$ in Table II. Unfortunately, the convergence of $-\beta \langle \delta U_{0s}^p \delta U_{ss}^p \rangle$ is very slow, especially for solvents with small dipolar strengths. In addition, the moment $-\beta \langle \delta U_{0s}^p \delta U_{ss}^p \rangle$ plotted against the number of trial

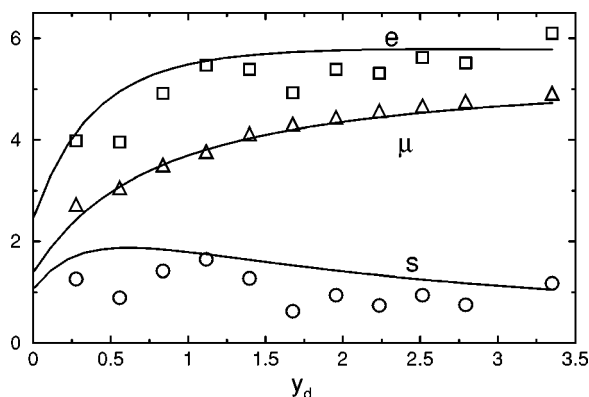


FIG. 3. $-\beta\mu_p$ (triangles), $-\beta u_p$ (squares), and $-s_p/k_B$ (circles) versus the solvent dipolar strength y_d . Solid lines indicate the PA for the chemical potential (μ), energy (e), and entropy (s) of solvation. Points indicate the simulation results; $r_{0s}=1.4$, $(Q^*)^2=0.5$, $\rho^*=0.8$.

moves shows relatively long plateaus that can easily be confused with stationary values. Therefore, only a qualitative analysis is feasible from the simulation data.

The internal energy of solvation becomes higher with increasing y_d , whereas the entropy of solvation changes slower (Fig. 3). This means that the solvation free energy in highly polar solvents is dominated by the solvation energy, whereas the entropic component is more important for solvation in quadrupolar solvents. This observation has an important bearing on the validity of continuum models of solvation in molecular liquids. The parameter χ_s [Eq. (24)] serves as a sensitive indicator of performance of linear response theories.^{10(c)} This is because for the LRA the chemical potential of solvation is quadratic in the solute dipole moment and χ_s is given by the equation

$$\chi_s = 1 - \left(y_d \frac{\partial}{\partial y_d} + y_q \frac{\partial}{\partial y_q} \right) \ln a(y_d, y_q), \quad (39)$$

where the response function $a(y_d, y_q)$ connects the solvation chemical potential and the squared solute dipole in the LRA,

$$\mu_p = -a(y_d, y_q) m_0^2. \quad (40)$$

All terms in the response function that are independent of the polarity parameters y_d and y_q disappear from the logarithmic derivative in Eq. (39). The parameter χ_s is thus affected only by the dependence of the response function on the dipolar and quadrupolar strengths. By calculating χ_s one can therefore extract the information about the solvent polarity dependence of the response function without complications due to geometric and other factors entering $a(y_d, y_q)$. The PA yields

$$\chi_s = \frac{f^{(3)}}{f^{(3)} + f^{(2)}}. \quad (41)$$

In the continuum Onsager treatment of dipole solvation, the solvent dependent part of the response function,

$$\frac{\epsilon(y_d, y_q) - 1}{2\epsilon(y_d, y_q) + 1}, \quad (42)$$

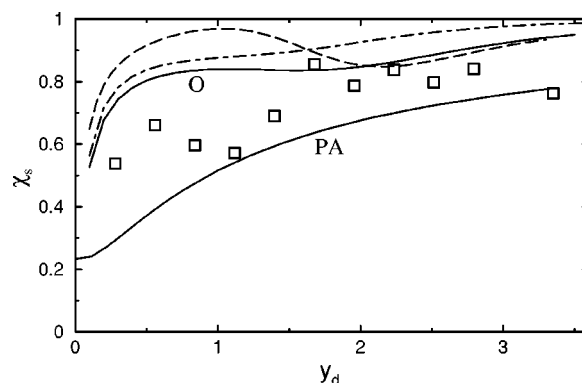


FIG. 4. Parameter χ_s calculated from the PA, and the continuum Onsager model (O). For the latter, the solid line indicates the calculation accounting for the dependence of the Kirkwood factor on y_d , the dash-dotted line is the Onsager approximation $g_K=1$, and the dashed line includes corrections for solvent quadrupoles according to Ref. 4(b). The dependence of the dielectric constant on y_d is taken from Ref. 10(c). Points are simulation results; $\rho^*=0.8$, $r_{0s}=1.4$, $(Q^*)^2=0.5$.

is given in terms of the solvent dielectric constant $\epsilon(y_d, y_q)$. The dependence of the dielectric constant on dipolar and quadrupolar densities follows from the Kirkwood equation,

$$\frac{[\epsilon(y_d, y_q) - 1][2\epsilon(y_d, y_q) + 1]}{9\epsilon(y_d, y_q)} = y_d g_K(y_d, y_q), \quad (43)$$

where the Kirkwood factor $g_K(y_d, y_q)$ depends on both y_d and y_q ,¹ although the dependence of g_K on y_q is generally unknown. In Fig. 4, the simulated χ_s is compared with the PA (labeled as ‘‘PA’’) and the continuum (labeled as ‘‘O’’) treatments. For the latter, two models for g_K , both disregarding the dependence on y_q , were employed. The solid line in Fig. 4 represents the calculation with $g_K(y_d)$ taken from our previous simulations of pure dipolar liquids^{10(c)} and the dash-dotted line indicates the Onsager approximation $g_K=1$. Also included is the parameter χ_s with the continuum response function taking into account the quadrupolar susceptibility (dashed line) recently proposed in Ref. 4(b).

The simulated χ_s falls in between the PA and continuum results (Fig. 4). Both the involvement of the quadrupolar susceptibility and the Onsager approximation $g_K=1$ worsen the agreement with simulations. Note that the Kirkwood factor g_K decays with y_q ¹ and an inclusion of its dependence on y_q would shift the χ_s curve upward.¹⁹ The PA does not give quantitatively correct energies and entropies of solvation resulting in underestimated values of the parameter χ_s . Note in this connection that the distinction between the continuum prediction and simulations for dipolar–quadrupolar liquids is not as dramatic as it was for purely dipolar solvents.^{10(c)} This is a reflection of a general trend of quadrupolar forces to break dipolar correlations in the solvent,^{1(b),2(b)} resulting in a better agreement with continuum theories. The gap between the simulated χ_s and its continuum estimate seems to broaden for smaller dipolar strengths. This is because the main shortcoming of continuum treatments of solvation is their failure to predict entropies of solvation. The increasing entropic character of solvation for quadrupolar fluids is

therefore the source of the increasing disagreement between the continuum solvation theory and simulations for smaller values of y_d .

V. CONCLUSIONS

We have used the Padé formulation of the perturbation expansion to treat solvation in dipolar–quadrupolar solvents. The standard version of the PA [Eq. (15)] gives overestimated solvation free energies, especially for the quadrupolar component of solvation. The difficulty was overcome by introducing empirical coefficients rescaling the three-particle perturbation integrals appearing in the perturbation expansion. Simulations with purely dipolar^{10(c)} and purely quadrupolar (Table I) solvents show that the corresponding empirical coefficients are independent of the solvent polarity and can be approximated by simple functions of the solute size. For solvents with nonzero dipoles and quadrupoles the correction parameter extracted from fitting the simulation data depends noticeably on y_d and y_q . It implies that the Padé form does not properly take into account the effect of interactions between solvent dipoles and solvent quadrupoles on solvation thermodynamics.

The proposed parameter κ_{qp} is solvent independent and enables us to fit the simulation data for the solute–solvent interaction energy. The deviation between the analytical equation and the simulated values for e_{0s} is less than the deviations between e_{0s} and $\beta\langle(\delta U_{0s}^p)^2\rangle$. This means that our linear response equation falls inside the uncertainties due to the nonlinear solvation effects (Fig. 2).

The interactions between the solvent dipoles and quadrupoles is the main factor determining the solvent reorganization energy. The reorganization energy e_{ss} is made by a compensation between a very large and positive correlator $-(\beta/2)\langle\delta U_{0s}^p U_{ss}^{DQ}\rangle$ and negative and smaller in absolute value correlators $-(\beta/2)\langle\delta U_{0s}^p U_{ss}^{DD}\rangle$ and $-(\beta/2)\langle\delta U_{0s}^p U_{ss}^{QQ}\rangle$. As a result, any errors in calculating the effect of dipole–quadrupole interactions in the solvent significantly impairs the accuracy of the energy and entropy of solvation. It is at this point where the main problem of the PA lies. As a result of this deficiency, the theory gives only approximate results for the energy and entropy of solvation (Figs. 3 and 4).

We should note, however, that these deficiencies concern only the total equilibrium energy and entropy of solvation. In spectroscopic applications, the reorganization energy of the solvent, e_{ss} , cancels out in the vertical energy gap and only the correct description of the solute–solvent solvation energy e_{0s} is necessary. For this purpose, the present theory is quite applicable. It gives the correct dependence of e_{0s} on the dipolar and quadrupolar densities, y_d and y_q . Since temperature explicitly comes only into these parameters, we can expect that thermochromic spectral coefficients may also be properly evaluated by using the Padé form.²⁰

ACKNOWLEDGMENTS

This research was supported by the Office of Naval Research (N00014-97-0265).

APPENDIX A: PERTURBATION INTEGRALS

The triple perturbation integrals in Eq. (14) read as

$$I_{DDD}^{(3)} = \frac{9}{4} \int_0^\infty \frac{dr}{r^2} \int_0^\infty \frac{dt}{t^2} \int_{|r-t|}^{r+t} \frac{ds}{s^2} g_{0ss}^{(0)}(r,t,s) W_{DDD}(r,t,s), \quad (\text{A1})$$

$$I_{DDQ}^{(3)} = \frac{3}{16} \int_0^\infty \frac{dr}{r^2} \int_0^\infty \frac{dt}{t^3} \int_{|r-t|}^{r+t} \frac{ds}{s^3} g_{0ss}^{(0)}(r,t,s) W_{DDQ}(r,t,s), \quad (\text{A2})$$

$$I_{DQQ}^{(3)} = \frac{5}{64} \int_0^\infty \frac{dr}{r^3} \int_0^\infty \frac{dt}{t^3} \int_{|r-t|}^{r+t} \frac{ds}{s^4} g_{0ss}^{(0)}(r,t,s) W_{DQQ}(r,t,s). \quad (\text{A3})$$

In Eqs. (A1)–(A3), $g_{0ss}^{(0)}(r,t,s)$ is the triple solute–solvent–solvent distribution function of the reference HS system. The angular factors $W_{DDD}(r,t,s)$, $W_{DDQ}(r,t,s)$, and $W_{DQQ}(r,t,s)$ are expressed in terms of the angles α_1 , α_2 , and α_3 in the vertices of the triangle with the sides r , t , and s formed by the solute and two solvent particles. They are given, according to Bell, by the relations^{5(a),21}

$$W_{DDD}(r,t,s) = 1 + 3 \cos \alpha_1 \cos \alpha_2 \cos \alpha_3, \quad (\text{A4})$$

$$W_{DDQ}(r,t,s) = 9 \cos \alpha_3 - 25 \cos 3\alpha_3 + 6 \cos(\alpha_1 - \alpha_2)(3 + 5 \cos 2\alpha_3), \quad (\text{A5})$$

$$W_{DQQ}(r,t,s) = 3(\cos \alpha_1 + 5 \cos 3\alpha_1) + 20 \cos(\alpha_2 - \alpha_3)(1 - 3 \cos 2\alpha_1) + 70 \cos 2(\alpha_2 - \alpha_3) \cos \alpha_1. \quad (\text{A6})$$

The triple perturbation integrals were calculated from simulated configurations of a HS solvent^{10(c),13} and by numerical integration in Eqs. (A1)–(A3). For the latter, the triple HS distribution function was taken in the superposition approximation,

$$g_{0ss}^{(0)}(r,t,s) = g_{0s}^{(0)}(r) g_{ss}^{(0)}(t) g_{0s}^{(0)}(s), \quad (\text{A7})$$

with the pair distribution functions $g_{0s}^{(0)}(r)$ and $g_{ss}^{(0)}(r)$ according to Lee and Levesque.²² Since the two procedures result in reasonably close values of the perturbation integrals (Fig. 5), we used numerical integration to fit the integrals to polynomials in the reduced density ρ^* and inverse solute size $1/r_{0s}$. The numerical data are fitted to the following relations:

$$I_6^{(2)} = \frac{a(\rho^*)}{r_{0s}^5} + \frac{b(\rho^*)}{r_{0s}^6} + \frac{c(\rho^*)}{r_{0s}^7} + \frac{d(\rho^*)}{r_{0s}^8}, \quad (\text{A8})$$

$$I_{DDQ}^{(3)} = \frac{a(\rho^*)}{r_{0s}^5} + \frac{b(\rho^*)}{r_{0s}^6} + \frac{c(\rho^*)}{r_{0s}^7} + \frac{d(\rho^*)}{r_{0s}^8}, \quad (\text{A9})$$

$$I_{DQQ}^{(3)} = \frac{a(\rho^*)}{r_{0s}^6} + \frac{b(\rho^*)}{r_{0s}^7} + \frac{c(\rho^*)}{r_{0s}^8} + \frac{d(\rho^*)}{r_{0s}^9}. \quad (\text{A10})$$

The functions $a(\rho^*)$, $b(\rho^*)$, $c(\rho^*)$, and $d(\rho^*)$ are, for each integral, polynomials of the third order in ρ^* with the coefficients listed in Table III. The coefficients in the density polynomials were fitted using the known $\rho^* \rightarrow 0$ limits,

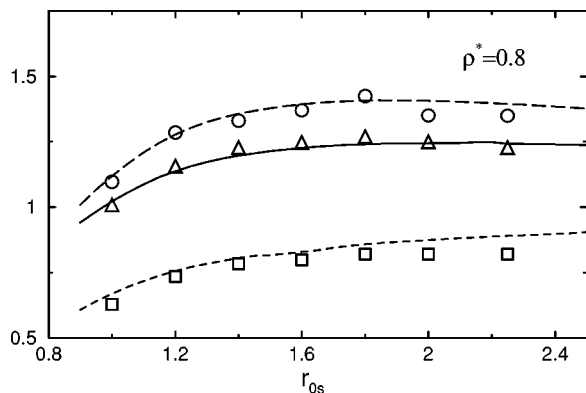


FIG. 5. Triple integrals $I_{\text{DDD}}^{(3)}$ (solid line, triangles), $I_{\text{DDQ}}^{(3)}$ (long-dashed line, circles), and $I_{\text{DQQ}}^{(3)}$ (short-dashed line, squares) versus r_{0s} at $\rho^*=0.8$. Points indicate the simulation data; lines correspond to calculations using the superposition approximation. The simulated data were obtained by extrapolating the simulation results at the finite solute concentration $x_0=1/(N+1)$ to the infinite system size with $x_0=0$. The number of particles in the simulation box was taken as $N=108, 255$, and 500 (Ref. 13).

$$I_6^{(2)} = \frac{1}{r_{0s}^5},$$

$$I_{\text{DDQ}}^{(3)} = \frac{4}{5r_{0s}^5} - \frac{1}{2r_{0s}^6} + \frac{1}{32r_{0s}^8},$$

$$I_{\text{DQQ}}^{(3)} = \frac{5}{24r_{0s}^6} - \frac{5}{64r_{0s}^8} + \frac{1}{128r_{0s}^{10}}.$$

APPENDIX B: SEPARATION OF THE AVERAGE SOLUTE-SOLVENT ENERGY INTO SOLVENT DIPOLAR AND QUADRUPOLAR COMPONENTS

The generating functional in Eq. (31) is the partition function of the potential $U(x,y)+U$ obtained by scaling the solvent dipole and quadrupole moments: $m \rightarrow xm$ and $Q \rightarrow yQ$. Under this scaling, the solute-solvent part of the multipolar potential becomes

$$u_{0s}^p(x,y) = (1+x)u_{0s}^{11} + (1+y)u_{0s}^{12}, \quad (\text{B1})$$

where u_{0s}^{11} and u_{0s}^{12} are given by Eqs. (3) and (4), respectively. For the solvent-solvent part of the potential $U(x,y)+U$, one has

$$u_{ss}^p = (1+x^2)u_{ss}^{11} + (1+xy)u_{ss}^{\text{DQ}} + (1+y^2)u_{ss}^{22}, \quad (\text{B2})$$

where u_{ss}^{11} , u_{ss}^{DQ} , and u_{ss}^{22} are the solvent-solvent multipolar potentials [Eqs. (7) and (8)].

The first expansion term (10) is bilinear in the solute-solvent potential. Therefore, $f^{(2)}(x,y)$ in Eq. (34) scales as $(1+x)^2$ and $(1+y)^2$, according to Eq. (B1). The second expansion term (14) is of the form $u_{0s}^p u_{ss}^p u_{0s}^p$ involving quadratic terms in the solute-solvent potential [factors $(1+x)^2$, $(1+y)^2$, and $(1+x)(1+y)$ in Eq. (35)] and linear in the components of the solvent-solvent potential (B2) [factors $(1+x^2)$, $(1+y^2)$, and $(1+xy)$ in Eq. (35)].

- ¹(a) G. N. Patey, D. Levesque, and J. J. Weis, *Mol. Phys.* **38**, 1635 (1979); (b) G. Stell, G. N. Patey, and J. S. Høye, *Adv. Chem. Phys.* **18**, 183 (1981).
- ²(a) J. Richardi, P. H. Fries, R. Fischer, S. Rast, and H. Krienke, *J. Mol. Liq.* **73-74**, 465 (1997); (b) P. H. Fries, J. Richardi, and H. Krienke, *Mol. Phys.* **90**, 841 (1997); (c) J. Richardi, C. Millot, and P. H. Fries, *J. Chem. Phys.* **110**, 1138 (1999).
- ³L. Reynolds, S. J. V. Frankland, M. L. Horng, and M. Maroncelli, *J. Phys. Chem.* **100**, 10337 (1996).
- ⁴(a) L. R. Evangelista and G. Barbero, *Phys. Lett. A* **185**, 213 (1994); (b) S. M. Chitanvis, *J. Chem. Phys.* **104**, 9065 (1996).
- ⁵(a) M. Flytzani-Stephanopoulos, K. E. Gubbins, and C. G. Gray, *Mol. Phys.* **30**, 1649 (1975); (b) G. N. Patey and J. P. Valleau, *J. Chem. Phys.* **64**, 170 (1976).
- ⁶The solvent reorganization energy of optical transitions becomes negative for such nonpolar solvents as benzene when the continuum response with nonzero quadrupolar susceptibility [Ref. 4(b)] is used in the calculations.
- ⁷(a) D. Chandler and H. C. Andersen, *J. Chem. Phys.* **57**, 1930 (1972); (b) F. Hirata and P. J. Rossky, *Chem. Phys. Lett.* **83**, 329 (1981); (c) B. M. Ladanyi and D. Chandler, *J. Chem. Phys.* **62**, 4308 (1975); (d) Y. Zhou, H. L. Friedman, and G. Stell, *Chem. Phys.* **152**, 185 (1991); (e) B.-C. Perng, M. D. Newton, F. O. Raineri, and H. L. Friedman, *J. Chem. Phys.* **104**, 7177 (1996); (f) S.-H. Chong and F. Hirata, *ibid.* **106**, 5225 (1997). (g) F. O. Raineri, B.-C. Perng, and H. L. Friedman, *Electrochim. Acta* **42**, 2749 (1997).
- ⁸C. G. Gray and K. E. Gubbins, *Theory of Molecular Fluids. V. 1: Fundamentals* (Clarendon, Oxford, 1984).
- ⁹(a) G. Stell, J. C. Rasaiah, and H. Narang, *Mol. Phys.* **23**, 393 (1972); (b) G. S. Rushbrooke, G. Stell, and J. S. Høye, *ibid.* **26**, 1199 (1973); (c) B. Larsen, J. C. Rasaiah, and G. Stell, *ibid.* **33**, 987 (1977); (d) G. Stell, in *Modern Theoretical Chemistry, V. 5. Part A. Equilibrium Techniques*, edited by B. J. Berne (Plenum, New York, 1977).
- ¹⁰(a) D. V. Matyushov and R. Schmid, *J. Chem. Phys.* **105**, 4729 (1996); (b) D. V. Matyushov and B. M. Ladanyi, *ibid.* **107**, 1362 (1997); (c) D. V. Matyushov and B. M. Ladanyi, *ibid.* **110**, 994 (1999).
- ¹¹(a) P. H. Fries and G. N. Patey, *J. Chem. Phys.* **82**, 429 (1985); (b) P. H. Lee and B. M. Ladanyi, *ibid.* **87**, 4093 (1987); (c) P. G. Kusalik and G. N. Patey, *ibid.* **88**, 7715 (1988).
- ¹²(a) F. Garisto, P. G. Kusalik, and G. N. Patey, *J. Chem. Phys.* **79**, 6294 (1983); (b) H.-A. Yu and M. Karplus, *ibid.* **89**, 2366 (1988). (c) N. M. Cann and G. N. Patey, *ibid.* **106**, 8165 (1997).
- ¹³D. V. Matyushov and B. M. Ladanyi, *J. Chem. Phys.* **107**, 5815 (1997).
- ¹⁴M. P. Allen and D. J. Tildesley, *Computer Simulation of Liquids* (Clarendon, Oxford, 1987).
- ¹⁵S. W. Leeuw, J. W. Perram, and E. R. Smith, *Annu. Rev. Phys. Chem.* **37**, 245 (1986).
- ¹⁶S. Jiang and K. S. Pitzer, *J. Chem. Phys.* **102**, 7632 (1995).
- ¹⁷(a) M. Bohn, J. Fischer, and J. M. Haile, *Mol. Phys.* **65**, 797 (1988); (b) C. Vega and K. E. Gubbins, *ibid.* **72**, 881 (1992); (c) G. S. Dubey and S. F. O'Shea, *Phys. Rev. E* **49**, 2175 (1994); (d) J. M. Polson and E. E. Burnell, *ibid.* **55**, 4321 (1997). (e) S. F. O'Shea, G. S. Dubey, and J. C. Rasaiah, *J. Chem. Phys.* **107**, 237 (1997).
- ¹⁸Higher order terms in m_0^2 can be included in a nonlinear Padé form [Refs. 10(b), 10(c)]. We, however, refrain from doing that in this paper, since already a linear response needs empirical corrections to fit the simulation data.
- ¹⁹According to the simulations by Patey and Valleau [Ref. 5(b)], $y_q(\partial \ln g_K / \partial y_q) \approx -0.1$ at $(m^*)^2 = 1.0$ and $(Q^*)^2 = 0.4$. A dependence of g_K on y_q is not, therefore, expected to modify considerably χ_s compared with the purely dipolar case $g_K(y_d)$.
- ²⁰The temperature evolution of absorption and emission maxima of optical transitions in acetonitrile as a solvent has been successfully analyzed within the Padé solvation model, P. Vath, M. B. Zimmt, D. V. Matyushov, and G. A. Voth, *J. Phys. Chem. B* (in press).
- ²¹(a) R. J. Bell, *J. Phys. B* **3**, 751 (1970); (b) J. C. Rasaiah and G. Stell, *Chem. Phys. Lett.* **25**, 519 (1974).
- ²²(a) L. Verlet and J.-J. Weis, *Phys. Rev. A* **5**, 939 (1972); (b) L. L. Lee and D. Levesque, *Mol. Phys.* **26**, 1351 (1973).